

Energy consumption and the unexplained winter warming over northern Asia and North America

Guang J. Zhang¹, Ming Cai^{2*} and Aixue Hu³

The worldwide energy consumption in 2006 was close to 498 exajoules. This is equivalent to an energy convergence of 15.8 TW into the populated regions, where energy is consumed and dissipated into the atmosphere as heat. Although energy consumption is sparsely distributed over the vast Earth surface and is only about 0.3% of the total energy transport to the extratropics by atmospheric and oceanic circulations, this anthropogenic heating could disrupt the normal atmospheric circulation pattern and produce a far-reaching effect on surface air temperature. We identify the plausible climate impacts of energy consumption using a global climate model. The results show that the inclusion of energy use at 86 model grid points where it exceeds 0.4 W m^{-2} can lead to remote surface temperature changes by as much as 1 K in mid- and high latitudes in winter and autumn over North America and Eurasia. These regions correspond well to areas with large differences in surface temperature trends between observations and global warming simulations forced by all natural and anthropogenic forcings¹. We conclude that energy consumption is probably a missing forcing for the additional winter warming trends in observations.

The emission of greenhouse gases from fossil-fuel burning, the land-use changes due to urbanization and deforestation, and anthropogenic aerosols are the most important anthropogenic factors that affect climate²⁻⁵. Anthropogenic greenhouse gases increase the surface temperature by trapping radiative energy emitted from the surface. Aerosols cool the Earth's surface by both directly scattering the sunlight and serving as condensation nuclei for clouds. Absorbing aerosols from fossil-fuel burning can also heat the atmosphere^{6,7}. Urbanization changes land surface properties (for example albedo, heat storage, surface roughness and moisture) and alters the surface energy balance and hydrological cycle locally, responsible for the so-called urban heat island (UHI) phenomenon in which an urban area is warmer than its surrounding rural areas⁸⁻¹¹. Another anthropogenic factor that has not been included in global warming climate model simulations and could have a significant climate effect is heating or thermal pollution from energy consumption^{12,13}.

Unlike anthropogenic greenhouse gases and aerosols, and land-use changes, which affect climate by altering the natural energy exchanges between the climate system and outer space and among different subcomponents of the climate system, the consumption of non-renewable energy itself represents a direct external energy source for the climate system because fossil-fuel burning releases energy sequestered millions of years ago. In large metropolitan areas with multimillions in population, a tremendous amount of energy

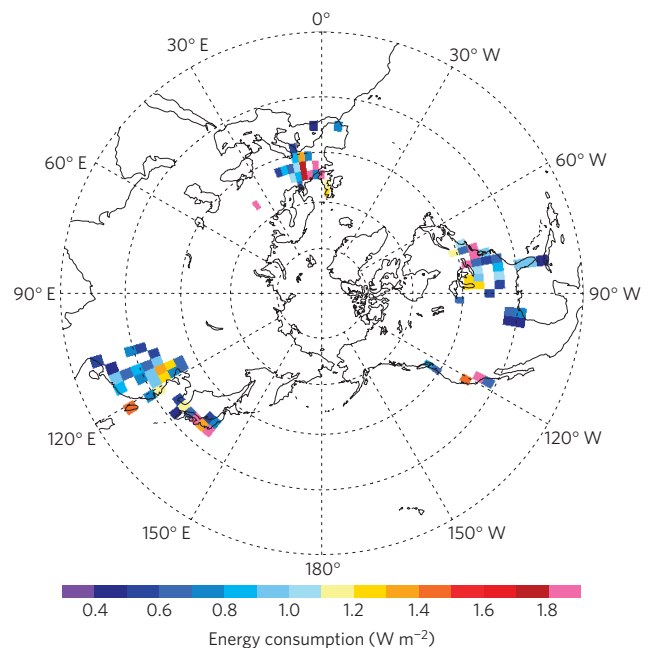


Figure 1 | Locations and area-averaged energy consumption of the 86 model grid points used in the perturbation runs. Each value is obtained by dividing the total estimated energy-use by the area represented by the model grid point.

is consumed each day. For example, energy consumption during the early morning hours of winter in the urban core of Tokyo is as high as $1,590 \text{ W m}^{-2}$ (ref. 14). Such an anthropogenic energy source can contribute significantly to the UHI effect, responsible for as much as 1 K warming in winter on top of the UHI effect due to changes in surface properties¹⁴⁻¹⁶.

Energy consumption is only about 0.3% of the 5 PW total energy transported across the 43° latitude to the extratropics by atmospheric and oceanic circulations¹⁷. However, this anthropogenic heating could disrupt the normal atmospheric circulation pattern and produce a far-reaching effect on regional and global climate. This idea was first brought forward almost half a century ago, but has been largely forgotten^{18,19}. Later work using a global climate model (GCM) found that the effect of energy consumption (or thermal pollution) is of the same order of magnitude as the model's natural fluctuations^{12,13}. However, it remains to be established whether the energy consumption would have a long-lasting effect

¹Scripps Institution of Oceanography, University of California San Diego, La Jolla, California 92093, USA, ²Department of Earth, Ocean, and Atmospheric Science, Florida State University, Tallahassee, Florida 32306, USA, ³Climate Change Research, CGD/NCAR, Boulder, Colorado 80307, USA.

*e-mail: mcai@fsu.edu.

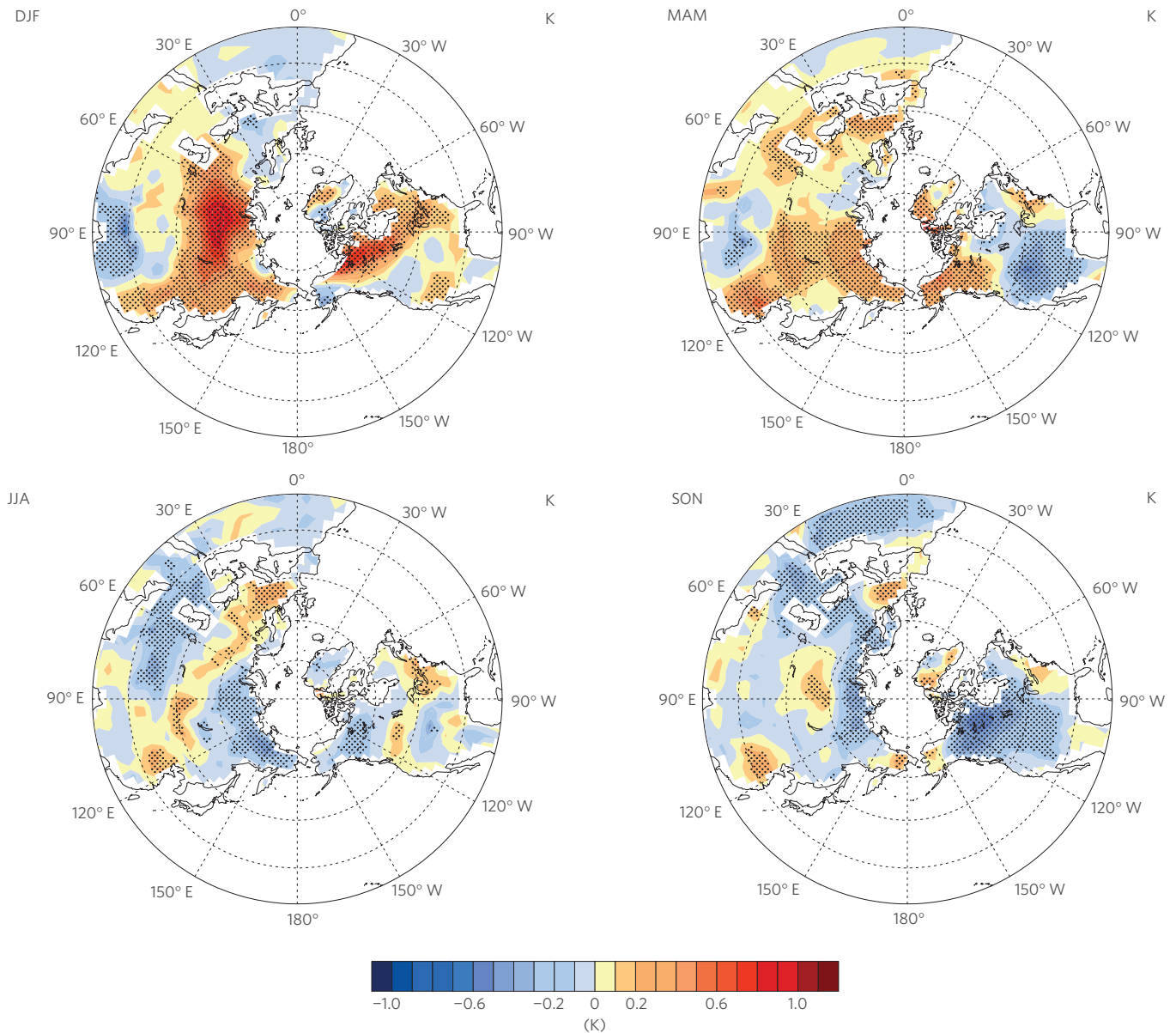


Figure 2 | Differences of seasonal mean surface air temperature between perturbation and control runs. The areas exceeding 95% *t*-test confidence level are stippled.

on the climate because the model integration in these GCM studies lasted only a few months. A regional model study has found that the anthropogenic heating could cause up to 0.5 K winter warming over western Europe²⁰. Here we use the National Center for Atmospheric Research (NCAR) Community Atmosphere Model CAM3 (ref. 21) to investigate the global-scale climate effect of energy consumption.

The control climate simulation is performed with the solar forcing that includes both diurnal and seasonal cycles, and the seasonally varying climatological sea surface temperature and sea ice from observations as the lower boundary conditions (see Supplementary Information for details). The model is run for 100 years using climatological forcing obtained from the time period 1981 to 2000, and we use the last 95 years to construct the annual cycle of the control run. The perturbation runs are performed by adding the energy consumption shown in Fig. 1 as a time-invariant heat source to the lowest model layer, which is about 130 m in thickness. We have performed five 100-year-long perturbation runs with different initial conditions derived from

the control integration. Again, the data from the first five years of each 100-year integration are excluded and the remaining 95 years are used in our analysis. The annual cycle derived from the control run is subtracted from each of the 95 years in each of the five perturbation runs, resulting in 475 monthly anomaly fields for each of the 12 calendar months. The ensemble mean of the 475 monthly anomalies is regarded as the difference between the perturbation and control runs, representing the climate response to the energy consumption forcing (Fig. 2). The ensemble mean of the differences between the perturbation and control runs becomes nearly unchanged when the ensemble member size is greater than 300 (Supplementary Fig. S1), implying that 475 ensemble members are enough for our purpose.

The global mean of energy consumption as an external energy source to our GCM climate simulations is 0.05 W m^{-2} , which is far less than the global mean ($\sim 1.5 \text{ W m}^{-2}$) of the present-day anthropogenic CO_2 forcing^{22,23}. Therefore, as expected, the global mean surface air temperature responses are insignificant for both the annual mean ($<0.01 \text{ K}$) and seasonal mean (for example, the

1981–2005 minus 1956–1980

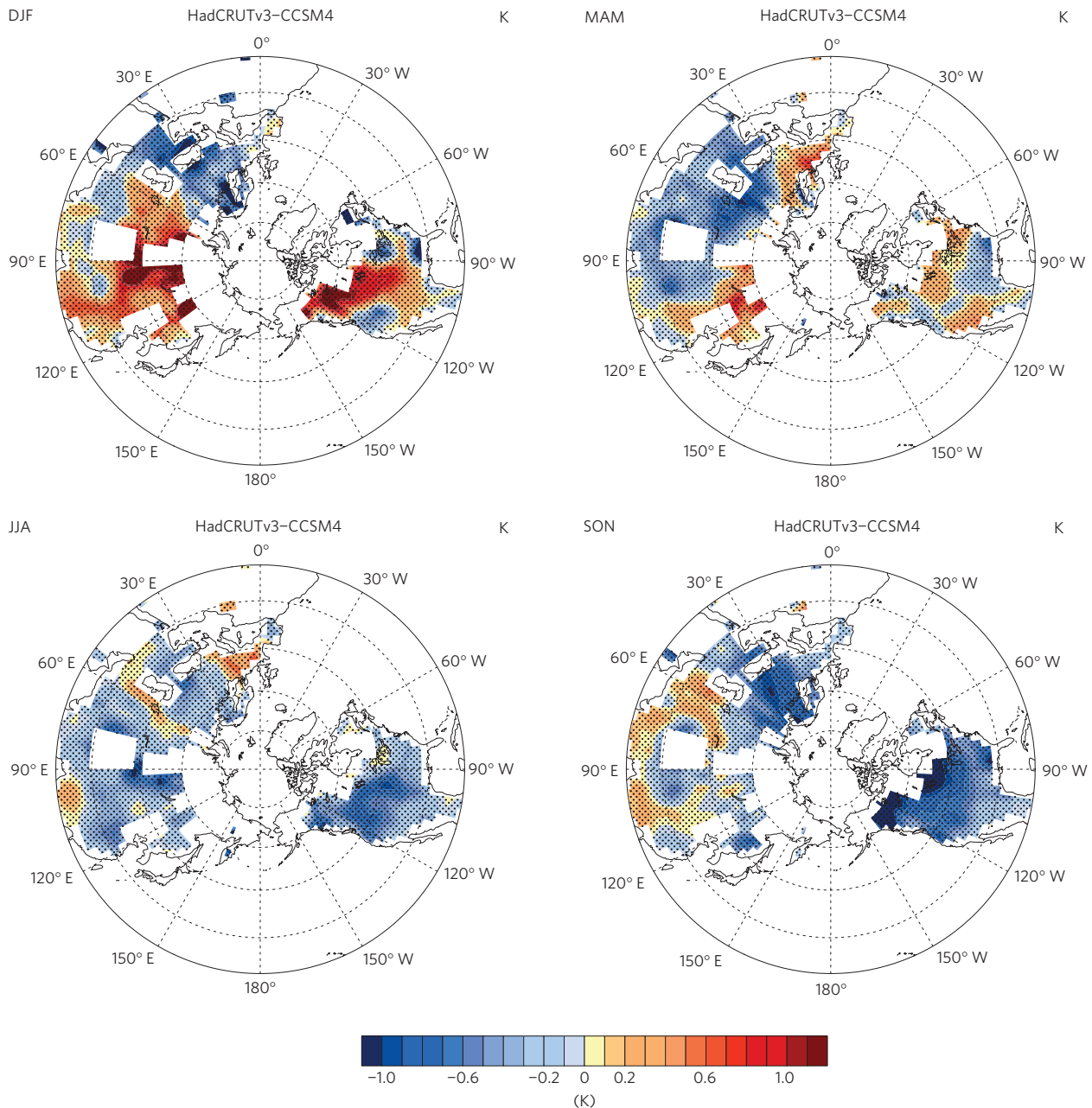


Figure 3 | Decadal land surface temperature trend differences between the HadCRUTv3 surface temperature observations and NCAR CCSM4 twentieth-century ensemble simulations. The trends in both the observation data set and the NCAR climate simulation data set are defined as the difference between the means of the periods 1981–2005 and 1956–1980 as in ref. 1. The blank areas over land are due to a lack of observed data for part of the period from 1956 to 2005 and the ocean data are masked out. Stippling shows that the decadal trends are statistically significant at the 95% confidence level in the CCSM4 twentieth-century simulations in comparison with the 1850 control run.

December–February (DJF) mean is only 0.02 K). However, there are statistically significant continental-scale warming and cooling of up to 1 K in mid- and high latitudes far away from the heat sources in DJF in response to the anthropogenic heating in the lowest model layer (Fig. 2). In the Eurasia continent, there is strong warming up to 1 K in Russia/northern Asia. Eastern China also experiences warming of up to 0.5 K. In North America, the northeastern US and southern Canada have significant warming, up to 0.8 K in the Canadian Prairies. Although the extra energy input imposed on the perturbation climate simulations is seasonally invariant, the surface air temperature responses are strongly season

dependent with the largest changes in boreal winter (DJF), followed by autumn (September–November (SON)) and spring (March–May (MAM)), and the smallest in boreal summer (June–August (JJA)). For example, whereas the DJF warming over northwestern Canada, eastern China, the Russian Arctic and the northeast of the US persists through the spring, the cooling in DJF over western Europe becomes warming in MAM. In SON, cooling is dominant and extensive, particularly in Russia, Canada and the US Midwest and warming primarily takes place in northern Europe. The weakest surface temperature response to energy consumption is in JJA, showing minor cooling over the region

around the Caspian Sea and warming over north Europe. The seasonal variation of the response to energy consumption indicates a shift in seasonality as DJF and MAM are dominated by warming whereas JJA and SON are dominated by cooling with little change in the annual mean temperature.

The surface temperature anomaly pattern for DJF has a high resemblance to the unexplained surface temperature trend in the second half of the twentieth century by anthropogenic radiative and aerosol forcing first identified in ref. 1. To establish any plausible link between the two, we have repeated the same analysis as in ref. 1 using the Hadley Centre Climate Research Unit version 3 surface temperature record and the NCAR Community Climate System Model version 4 (CCSM4) twentieth-century climate simulations (see Supplementary Information for details). Indeed, the NCAR CCSM4 twentieth-century climate simulations forced by all natural and anthropogenic forcing agents also exhibit similar unexplained surface temperature trend patterns (Fig. 3) as those shown in ref. 1. For example, the observed DJF warming is larger than the GCM simulated warming in Eurasia and North America. There is a large degree of similarity between Figs 2 and 3, particularly in the winter season when both the surface temperature response to energy consumption and the unexplained surface temperature trends are largest. The spatial anomaly correlations in DJF, MAM, JJA and SON over the statistically significant regions are 0.52, 0.11, 0.22 and 0.60, respectively. In particular, the unexplained DJF warming over eastern China, northern Asia/Russia, northeastern and southwestern US, and southern Canada, and cooling over northwestern US, northern Africa, the Mediterranean and western Europe are well captured by the surface temperature changes in response to energy consumption. The unexplained surface temperature trends in the other three seasons are also fairly correlated with the surface temperature changes in response to energy consumption, with exceptions over the central Eurasian continent in MAM and central China and the US in JJA. Furthermore, the seasonal variation of the unexplained surface temperature changes in observations also exhibits a similar shift in seasonality to that in response to energy consumption, namely, the general warming in DJF and MAM and cooling in JJA and SON. Therefore, it is likely that energy consumption is a plausible missing source for the unexplained surface temperature trends in observations and may have contributed to the observed surface warming in winter in high latitudes of northern Asia and North America, on top of the warming due to anthropogenic radiative and aerosol forcing.

There is also a robust change in atmospheric circulation in response to the anthropogenic heating due to energy consumption. There is an equatorward shift of the winter mid-latitude jet, with increasing westerly wind at 20° N and decreasing westerly wind at 40° N. In addition, the westerly wind at high latitudes (60° N) is strengthened in the upper troposphere (Supplementary Fig. S2). These changes are consistent with the thermal wind relationship with warming in mid- and high latitudes and cooling south of 40° N. Note that the energy consumption is mostly concentrated in the mid-latitude belt (Fig. 1). The DJF mean zonal wind change in response to it is similar to the findings from idealized GCM simulations with thermal forcing localized in mid-latitudes²⁴.

The heating-induced changes in the pressure field disrupt the normal atmospheric general circulation in the winter season, responsible for the continental-scale pattern of surface temperature changes in mid- and high latitudes in DJF. The anomalous low-pressure centre in the Russian Arctic and high pressure in central Asia (Supplementary Fig. S3) produce southerly wind anomalies in a region from 50° to 70° N and 60° to 90° E (Fig. 4a). These southerly wind anomalies advect warm air from the south, resulting in a centre of warm surface temperature anomalies there. Similarly, the warm anomalies in the Canadian Prairies and Northwest Territories are a result of advection of warm air from

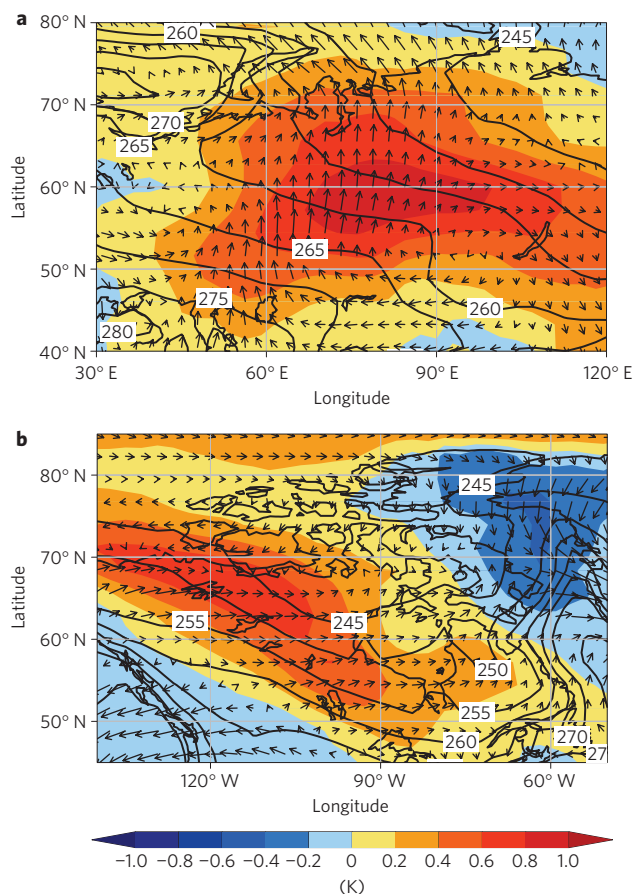


Figure 4 | Surface air temperature in DJF from the control run and differences in surface wind and temperature between the perturbation and control runs. a, b, Horizontal temperature advection in warm and cold anomaly regions for central Asia (a) and Canada and northwestern Greenland (b). Contours indicate the surface air temperature (K) from the control run, shading highlights the temperature differences, and vectors show anomalies in surface winds.

the northeastern Pacific and western Canada by anomalous westerly and southwesterly wind. The cold surface temperature anomalies in the northeastern Canadian Arctic, Baffin Bay and northwestern Greenland are a result of cold advection of the Arctic air (Fig. 4b) by the anomalous northerly flow to the west of the anomalous low-pressure centre in Greenland (Supplementary Fig. S3).

To put our results in perspective, we note that a doubling of CO₂ can cause regional surface temperature changes of as much as 6 K, whereas land-cover changes due to deforestation in an Intergovernmental Panel on Climate Change global-change scenario can cause up to 2 K regional surface temperature change³. In response to anthropogenic heating resulting from energy consumption, high-latitude regions of Eurasia can be warmed by as much as 1 K, and the northeastern US and the Canadian Prairies and Northwest Territories can be warmed by up to 0.6 K. Our modelling results are robust because this continental-scale temperature change pattern already emerges in an *n*-member ensemble mean with *n* > 100 and it remains unchanged when the ensemble member size is above 300 (Supplementary Fig. S1). We note that these results are from one model, and they could be model dependent.

Our demonstration of the continental-scale climate response to anthropogenic heating from energy use and its resemblance to the unexplained surface temperature changes strongly suggest the need to include energy consumption, in addition to anthropogenic greenhouse gases, aerosols and land-use changes, in climate

simulations for future climate-change projections. The estimate of energy consumption for each grid point is based on country-by-country energy consumption data. As such, we may have underestimated the energy consumption in cities, particularly in developing countries where energy use per capita in cities is far greater than the national average. Furthermore, the energy consumption included in our GCM experiments is conservative (about 42% of the total world energy consumption). Thus, the actual climate impact of energy consumption could be larger than reported in this study. A better and more accurate estimate of global energy use based on city-by-city information should be developed to fully account for the climate impact due to energy consumption in future climate-change projections.

Methods

We estimate the total energy use at each model grid point using the average energy consumption rate per capita in 2006 for each country published in ref. 25, which is available for download at <http://www.eia.doe.gov/emeu/international/energyconsumption.html>. The worldwide energy consumption total in 2006 was 472.4×10^{15} Btu, which is about 498 exajoules using the conversion rate of 1 Btu = 1,054.35 J. The population data were published in 2005 Gridded Population of the World: Future Estimates (GPWFE), available for download at <http://sedac.ciesin.columbia.edu/gpw>. The energy consumption rate at each model grid point is estimated as the product of the population at that grid point and the average energy consumption rate per capita for the country where the model grid is located.

The energy consumption rate can also be estimated from a conversion of carbon emission data, such as inventories of fossil-fuel combustion developed in ref. 26 and population-based carbon emission data developed in ref. 27. The carbon emission data from ref. 26 include fossil-fuel combustion from industrial, electricity production, transportation, commercial and residential sectors. As different types of fossil fuel have different emission factors, there is a large range in carbon emission inventory uncertainties. To convert energy consumption rate to carbon emission rate, we use an approximate conversion factor, namely that the total energy consumption in one year over 100 km^2 at the rate of 1 W m^{-2} is equivalent to a carbon emission rate of $1.9 \log_{10}(\text{GgC})$ per 100 km^2 per year or 81.9 k ton carbon per year and per 100 km^2 . Our energy consumption rate estimate falls within the range of those from fossil-fuel combustion of refs 26,27.

To avoid a potential exaggeration of the effect of energy consumption on climate, we consider only the GCM grid points where energy consumption exceeds 0.4 W m^{-2} . As a result, those energy consumption data whose accuracy and spatial variation are subject to large uncertainties are excluded in our climate simulations. There are a total of 86 grid points that meet the criterion, and they are all in North America, East Asia and Europe, as shown in Fig. 1. In our modelling experiments, the area-averaged energy consumption rates in Fig. 1 are added to the temperature equation in the lowest GCM model layer as an extra heating term representing the anthropogenic heating. This is equivalent to assuming that 100% of the energy consumed is used to heat the boundary layer atmosphere locally and immediately. The area covered by these 86 grid points is about 6.5 million square kilometres, or 1.27% of the total Earth surface. However, their combined energy consumption is $6.67 \times 10^{12} \text{ W}$, about 42.2% of the total energy consumption worldwide.

As we consider only megacities with large energy consumption, the climate response to this anthropogenic energy source may be in the lower bound of the plausible climate impact from the world's energy consumption. The anthropogenic heating can be in the form of either ground heat flux, sensible heat flux or long-wave radiation. Ground heat flux directly heats the surface, which in turn radiates more energy upwards and produces stronger surface sensible heat fluxes. The emitted long-wave radiation, on the other hand, can be absorbed at the surface and above. As the atmosphere is highly opaque to long-wave radiation, most of the thermal energy emitted from the surface would be trapped in the lower troposphere and heat the air there, in much the same way as sensible heat. Thus, as in other studies^{12,13}, the anthropogenic heat source is treated as sensible heat in our numerical simulations.

Received 16 August 2012; accepted 7 December 2012;
published online 27 January 2013

References

1. Knutson, T. R. *et al.* Assessment of twentieth-century regional surface temperature trends using the GFDL CM2 coupled models. *J. Clim.* **19**, 1624–1651 (2006).
2. Trenberth, K. E. *et al.* in *IPCC Climate Change: The Physical Science Basis* (eds Solomon, S. *et al.*) 235–336 (Cambridge Univ. Press, 2007).
3. Ramanathan, V., Crutzen, P. J., Kiehl, J. T. & Rosenfeld, D. Aerosols, climate, and the hydrological cycle. *Science* **294**, 2119–2124 (2001).
4. Feddema, J. J. *et al.* The importance of land-cover change in simulating future climates. *Science* **310**, 1674–1678 (2005).

5. Rosenfeld, D. *et al.* Flood or drought: How do aerosols affect precipitation? *Science* **321**, 1309–1313 (2008).
6. Ramanathan, V. *et al.* Warming trends in Asia amplified by brown cloud solar absorption. *Nature* **448**, 575–578 (2007).
7. Ramanathan, V. & Carmichael, G. Global and regional climate changes due to black carbon. *Nature Geosci.* **1**, 221–227 (2008).
8. Landsberg, H. E. *The Urban Climate* (Academic, 1981).
9. Oke, T. R. The energetic basis of the urban heat island. *Q. J. R. Meteorol. Soc.* **108**, 1–24 (1982).
10. Bornstein, R. & Lin, Q. Urban heat islands and summertime convective thunderstorms in Atlanta: Three case studies. *Atmos. Environ.* **34**, 507–516 (2000).
11. Shepherd, J. M., Pierce, H. & Negri, A. J. Rainfall modification by major urban areas: Observations from spaceborne rain radar on the TRMM satellite. *J. Appl. Meteorol.* **41**, 689–701 (2002).
12. Washington, W. M. Numerical climate-change experiments: The effect of man's production of thermal energy. *J. Appl. Meteorol.* **11**, 769–772 (1972).
13. Washington, W. M. & Chervin, R. M. Regional climatic effects of large-scale thermal pollution simulation studies with the NCAR general circulation model. *J. Appl. Meteorol.* **18**, 1501–1511 (1979).
14. Ichinose, T., Shimodozono, K. & Hanaki, K. Impact of anthropogenic heat on urban climate in Tokyo. *Atmos. Environ.* **33**, 3897–3909 (1999).
15. Kusaka, H. & Kimura, F. Thermal effects of urban canyon structure on the nocturnal heat island: Numerical experiment using a mesoscale model coupled with an urban canopy model. *J. Appl. Meteorol.* **43**, 1899–1910 (2004).
16. Oleson, K. W., Bonan, G. B., Feddema, J. & Jackson, T. An examination of urban heat island characteristics in a global climate model. *Int. J. Climatol.* **31**, 1845–1865 (2011).
17. Trenberth, K. E. & Caron, J. M. Estimates of meridional atmosphere and ocean heat transports. *J. Clim.* **14**, 3433–3443 (2001).
18. Budyko, M., Drosdov, I. O. A. & Yudin, M. I. Influence of economic activity on climate. *Modern Problems of Climatology* (Collection of Articles), FTD-HT-23-1338-67 (USAF, 1966).
19. Sellers, W. D. Global climatic model based on the energy balance of the Earth-atmosphere system. *J. Appl. Meteorol.* **8**, 392–400 (1969).
20. Block, A., Keuler, K. & Schaller, E. Impacts of anthropogenic heat on regional climate patterns. *Geophys. Res. Lett.* **31**, L12211 (2004).
21. Collins, W. D. *et al.* The formulation and atmospheric simulation of the Community Atmosphere Model version 3 (CAM3). *J. Clim.* **19**, 2144–2161 (2006).
22. *IPCC Climate Change 2007: The Scientific Basis* (eds S. Solomon *et al.*) (Cambridge Univ. Press (2007).
23. Hansen, J., Sato, M. & Ruedy, R. Radiative forcing and climate response. *J. Geophys. Res.* **102**, 6831–6864 (1997).
24. Ring, M. J. & Plumb, R. A. The response of a simplified GCM to axisymmetric forcings: Applicability of the fluctuation-dissipation theorem. *J. Atmos. Sci.* **65**, 3880–3898 (2008).
25. International Energy Agency, World Energy Demand and Economic Outlook. *International Energy Outlook 2009*, 7–20 (2009).
26. Gurney, K. *et al.* High resolution fossil fuel combustion CO₂ emission fluxes for the United States. *Environ. Sci. Technol.* **43**, 5535–5541 (2009).
27. Rayner, P. J., Raupach, M. R., Paget, M., Peylin, P. & Koffi, E. A new global gridded data set of CO₂ emissions from fossil fuel combustion: Methodology and evaluation. *J. Geophys. Res.* **115**, D19306 (2010).

Acknowledgements

This research was in part supported by the National Science Foundation (ATM-0833001 and ATM-0832915), the Office of Science (BER), the US Department of Energy Regional and Global Climate Modelling programme (DE-SC0004974) and Atmospheric System Research programme (DE-SC0000805), and the NOAA CPO/CPA programme (NA10OAR4310168). Portions of this study were also supported by the DOE Cooperative Agreement No. DE-FC02-97ER62402, and the National Science Foundation. The NCAR is sponsored by the National Science Foundation.

Author contributions

M.C. conceived the study with G.J.Z. M.C. compiled the global energy consumption data. G.J.Z. performed the numerical simulations and analysed model output. Both G.J.Z. and M.C. interpreted the results and wrote the paper. A.H. analysed the surface temperature trend differences between observations and CCSM4 global warming simulations, and contributed to revising the paper.

Additional information

Supplementary information is available in the [online version of the paper](#). Reprints and permissions information is available online at www.nature.com/reprints. Correspondence and requests for materials should be addressed to M.C.

Competing financial interests

The authors declare no competing financial interests.